

We are IntechOpen, the world's leading publisher of Open Access books Built by scientists, for scientists

6,900

Open access books available

186,000

International authors and editors

200M

Downloads

Our authors are among the

154

Countries delivered to

TOP 1%

most cited scientists

12.2%

Contributors from top 500 universities



WEB OF SCIENCE™

Selection of our books indexed in the Book Citation Index
in Web of Science™ Core Collection (BKCI)

Interested in publishing with us?
Contact book.department@intechopen.com

Numbers displayed above are based on latest data collected.
For more information visit www.intechopen.com



Transient Pressure and Pressure Derivative Analysis for Non-Newtonian Fluids

Freddy Humberto Escobar

Additional information is available at the end of the chapter

<http://dx.doi.org/10.5772/50415>

1. Introduction

Conventional well test interpretation models do not work in reservoirs containing non-Newtonian fluids such as completion and stimulation treatment fluids: polymer solutions, foams, drilling muds (this should not be considered as a reservoir fluid, since before testing we should clean the well to remove all the drilling invasion fluids, however it obeys the power-law), etc., and some paraffinic oils and **heavy crude oils**. Non-Newtonian fluids are generally classified as time independent, time dependent and viscoelastic. Examples of the first classification are the Bingham, pseudoplastic and dilatant fluids, Figure 1, which are commonly dealt by petroleum engineers.

As a special kind of non-Newtonian fluid, Bingham fluids (or plastics) exhibit a finite yield stress at zero shear rates. There is no gross movement of fluids until the yield stress, τ_y , is exceeded. Once this is accomplished, it is also required cutting efforts to increase the shear rate, i.e. they behave as Newtonian fluids. These fluids behave as a straight line crossing the y axis in $\tau = \tau_y$, when the shear stress, τ plotted against the shear rate, γ in Cartesian coordinates. The characteristics of these fluids are defined by two constants: the yield, τ_y , which is the stress that must be exceeded for flow to begin, and the Bingham plastic coefficient, μ_B . The rheological equation for a Bingham plastic is,

$$\tau = \tau_y + \mu_B \gamma'$$

The Bingham plastic concept has been found to approximate closely many real fluids existing in porous media, such as paraffinic oils, heavy oils, drilling muds and fracturing fluids, which are suspensions of finely divided solids in liquids. Laboratory investigations have indicated that the flow of heavy-oil in some fields has non-Newtonian behavior and approaches the Bingham type.

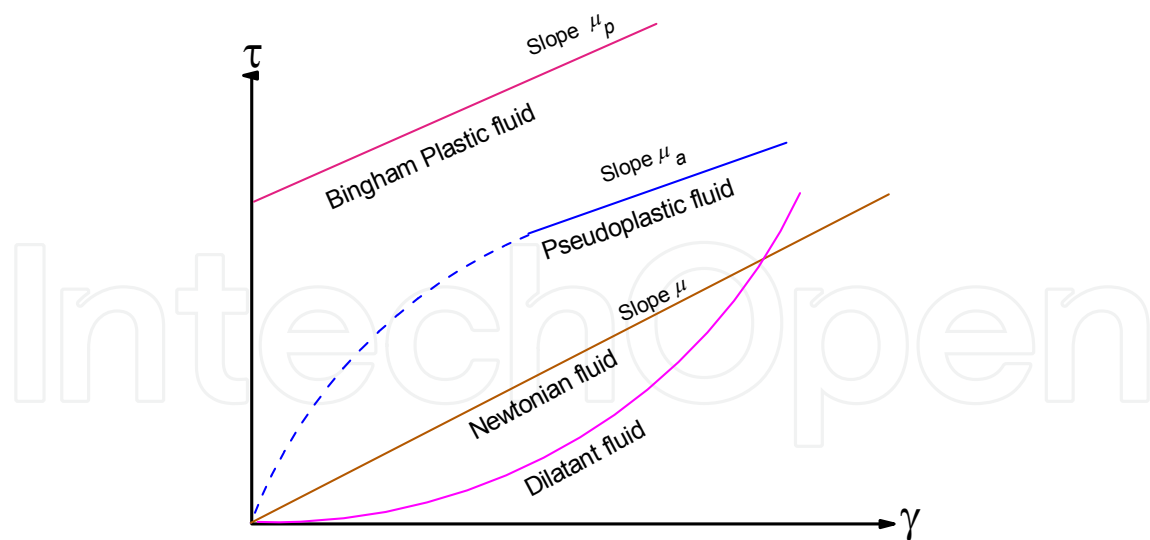


Figure 1. Schematic representation of time-independent fluid

Pseudoplastic and dilatant fluids have no yield point. The slope of shear stress versus shear rate decreases progressively and tends to become constant for high values of shear stress for pseudoplastic fluids. The simplest model is power law,

$$\tau = k\gamma^n; \quad n < 1.$$

k and n are constants which differ for each particular fluid. k measures the flow consistency and n measures the deviation from the Newtonian behavior which $k = \mu$ and $n = 1$.

Dilatant fluids are similar to pseudoplastic except that the apparent viscosity increases as the shear stress increases. The power-law model also describes the behavior of dilatant fluids but $n > 1$.

Currently, unconventional reservoirs are the most impacting subject in the oil industry. Shale reservoirs, coalbed gas, tight gas, gas hydrates, gas storage, geothermal energy, coal – conversion to gas, coal-to-gas, in-situ gasification and heavy oil are considered unconventional reservoirs. In the field of well testing, several analytical and numerical models taking into account Bingham, pseudoplastic and dilatant non-Newtonian behavior have been introduced in the literature to study their transient nature in porous media for a better reservoir characterization. Most of them deal with fracture wells, homogeneous and double-porosity formations and well test interpretation is conducted via the straight-line conventional analysis or type-curve matching and recently some studies involving the pressure derivative have also been introduced.

When it is required to conduct a treatment with a non-Newtonian fluid in an oil-bearing formation, this comes in contact with conventional oil which possesses a Newtonian nature. This implies the definition of two media with entirely different mobilities. If a pressure test is run in such a system, the interpretation of data from such a test through the use of conventional straight-line method may be erroneous and may not provide a way for verification of the results obtained.

The purpose of this chapter is to provide the most updated state-of-the-art on transient analysis of Non-Newtonian fluids and to present both conventional and modern methodologies for well test interpretation in reservoirs saturated with such fluids. Especial interest is given to the use of the pressure and pressure derivative for both homogeneous and double-porosity formations.

2. Non-Newtonian fluids in transient pressure analysis

Non-Newtonian fluids are often used during various drilling, workover and enhanced oil recovery processes. Most of the fracturing fluids injected into reservoir-bearing formations behave non-Newtonianly and these fluids are often approximated by Newtonian fluid flow models. In the field of well testing, several analytical and numerical models taking into account Bingham and pseudoplastic non-Newtonian behavior have been introduced in the literature to study the transient nature of these fluids in porous media for a better reservoir characterization. Most of them deal with fracture wells and homogeneous formations and well test interpretation is conducted via the straight-line conventional analysis or type-curve matching. Only a few studies consider pressure derivative analysis. However, there exists a need of a more practical and accurate way of characterizing such systems.

Many studies in petroleum and chemical engineering and rheology have focused on non-Newtonian fluid behavior through porous formations, among them, we can name [6, 9, 10, 18, 20, 23]. Several numerical and analytical models have been proposed to study the transient behavior of non-Newtonian fluid in porous media. Since all of them were published before the eighties, when the pressure derivative concept was inexistent; interpretation technique was conducted using either conventional analysis or type-curve matching.

It is worth to recognize that Ikoku has been the researcher who has contributed the most to non-Newtonian power-law fluids modeling, as it is demonstrated in the works of [9,10,11,13]. All of these models have been used later for other researchers for further development of test interpretation techniques. For instance, reference [24] presented a study of a pressure fall-off behavior after the injection of a non-Newtonian power-law fluid. [14] presented a study using the elliptical flow on transient analysis interpretation in Polymer flooding EOR since polymer solutions also exhibit non-Newtonian rheological behavior such as in-situ shear-thinning and shear-thickening effects.

[25] used for the first time the pressure-derivative concept for well test analysis of non-Newtonian fluids, and later on, [12] presented the first extension of the *TDS* (Tiab's Direct Synthesis) technique, [21] to non-Newtonian fluids. [7] used type-curve matching for interpretation of pressure test for non-Newtonian fluids in infinite systems with skin and wellbore storage effects. Recent applications of the derivative function to non-Newtonian system solutions are presented by [1] and [15] who applied the *TDS* technique to radial composite reservoirs with a Non-Newtonian/Newtonian interface for pseudoplastic and dilatants systems, respectively.

As far as non-Newtonian fluid flow through naturally fractured reservoirs is concerned only a study presented by [19] is reported in the literature. He presented the analytical solution for the transient behavior of double-porosity infinite formations which bear a non-Newtonian pseudoplastic fluid and his analytical solution also considers wellbore storage effects and skin factor; therefore, [2] used the analytical solution without wellbore storage and skin introduced by [19] was used to develop an interpretation technique using the pressure and pressure derivative, so expressions to estimate the Warren and Root parameters [26] (dimensionless *storage coefficient and interporosity flow parameter*) were found and successfully tested with synthetic data.

3. Pseudoplastic infinite-acting radial flow regime in homogeneous formations

Interpretation of pressure tests for non-Newtonian fluids is performed differently to conventional Newtonian fluids. During radial flow regime, Non-Newtonian fluids exhibit a pressure derivative curve which is not horizontal but rather inclined. As shown by [12], the smaller the value of n (flow behavior index) the more inclined is the infinite-acting pressure derivative line, see Figure 2.

A partial differential equation for radial flow of non-Newtonian fluids that follow a power-law relationship through porous media was proposed [11]. Coupling the non-Newtonian Darcy's law with the continuity equation, they derived a rigorous partial differential equation:

$$\frac{\partial^2 P}{\partial r^2} + \frac{n}{r} \frac{\partial P}{\partial r} = c_t \phi n \left(\frac{\mu_{eff}}{k} \right)^{1/n} \left(-\frac{\partial P}{\partial r} \right)^{(n-1)/n} \frac{\partial P}{\partial t} \quad (1)$$

This equation is nonlinear. For analytical solutions, a linearized approximation was also derived by [11]:

$$\frac{1}{r^n} \frac{\partial}{\partial r} \left(r^n \frac{\partial P}{\partial r} \right) = G r^{1-n} \frac{\partial P}{\partial t} \quad (2)$$

Where:

$$G = \frac{3792.188 n \phi c_t \mu_{eff}}{k} \left(96681.605 \frac{h}{qB} \right)^{1-n} \quad (3)$$

and,

$$\mu_{eff} = \left(\frac{H}{12} \right) \left(9 + \frac{3}{n} \right)^n \left(1.59344 \times 10^{-12} k \phi \right)^{(1-n)/2} \quad (4)$$

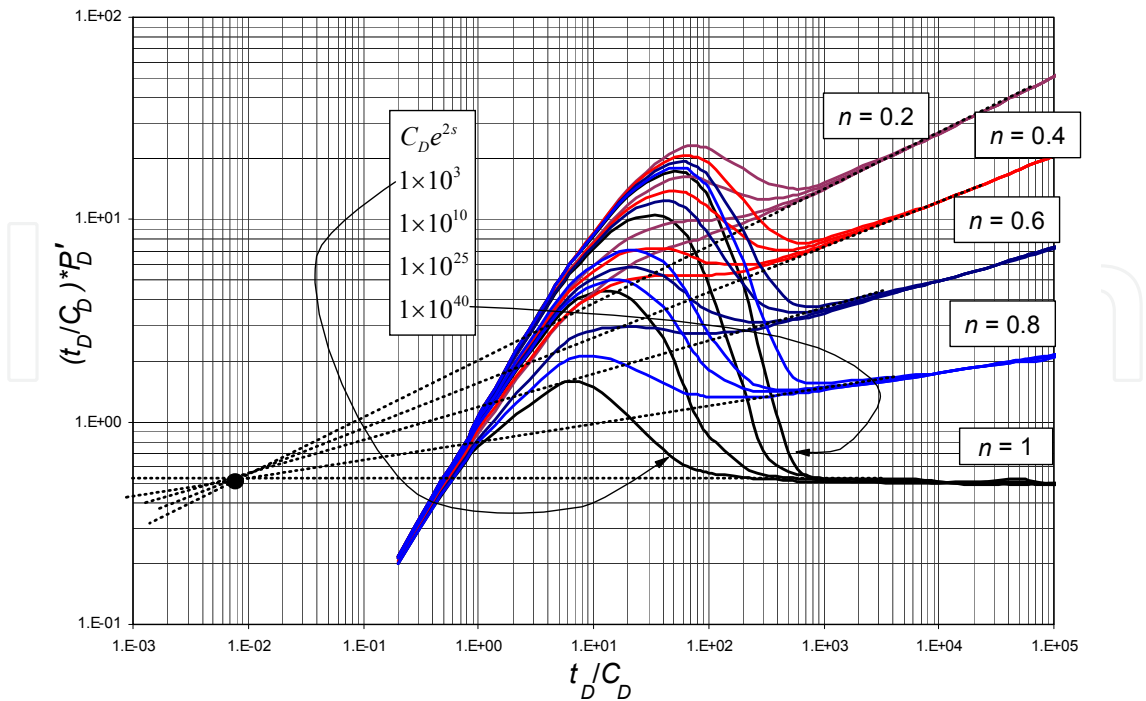


Figure 2. Pressure derivative for a pseudoplastic non-Newtonian fluid in an infinite reservoir – After Reference [12]

The dimensionless quantities were also introduced by [10] as

$$P_{DNN} = \frac{\Delta P}{141.2(96681.605)^{1-n} \left(\frac{qB}{h}\right)^n \frac{\mu_{eff} r_w^{1-n}}{k}} \tag{5}$$

$$t_{DNN} = \frac{t}{Gr_w^{3-n}} \tag{6}$$

$$P_{DN} = \frac{k h \Delta P}{141.2 q \mu_N B} \tag{7}$$

$$t_{DN} = \frac{0.0002637 k t}{\phi \mu_N c_t r_w^2} \tag{8}$$

$$r_D = \frac{r}{r_w} \tag{9}$$

Where suffix *N* indicates Newtonian and suffix *NN* indicates non-Newtonian. The dimensionless well pressure analytical solution in the Laplace space domain for the case of a well producing a pseudoplastic non-Newtonian fluid at a constant rate from an infinite reservoir is given in reference [11]:

$$\bar{P}_D(\tilde{s}) = \frac{K_\nu \left(\beta \sqrt{\tilde{s}} r_D^{1/\beta} \right) + s \sqrt{\tilde{s}} K_\beta \left(\beta \sqrt{\tilde{s}} \right)}{\tilde{s} \left(\sqrt{\tilde{s}} K_\beta \left(\beta \sqrt{\tilde{s}} \right) + \tilde{s} C_D \left[K_\nu \left(\beta \sqrt{\tilde{s}} \right) + s \sqrt{\tilde{s}} K_\beta \left(\beta \sqrt{\tilde{s}} \right) \right] \right)} \quad (10)$$

Being $\beta = 2/(3-n)$ and $\nu = (1-n)/(3-n)$.

The dimensionless pressure derivative during radial flow regime is governed by:

$$\left(t_D^* P_D' \right)_{r_{NN}} = 0.5 t_{DNN}^\alpha \quad (11)$$

[12] presented the following expression to estimate the permeability,

$$\frac{k}{\mu_{eff}} = \left[0.5 \frac{t_r^\alpha}{C^\alpha (t^* \Delta P')_r} \frac{(2\pi h)^{n(\alpha-1)} r_w^{(1-n)(1-\alpha)}}{q^{n(\alpha-1)-\alpha}} \right]^{1-\alpha} \quad (12)$$

where $\alpha = -0.1486n^2 - 0.178n + 0.3279$

being n the flow behavior index which may be found from the slope of the pressure derivative curve during radial flow regime. [12] also introduced another expressions and correlations to find permeability, skin factor and wellbore storage coefficient using the maximum point (peak) found on the pressure derivative curve during wellbore storage effects which are not shown here. The point of intercept between the early unit-slope line and radial flow regime is used to estimate wellbore storage:

$$t_i = \frac{(3.13e^{-1.85n}) C \mu_{eff}}{(2\pi h)^n k} \left(\frac{q}{r_w} \right)^{n-1} \quad (13)$$

Parameters in both Equations 11 and 12 are given in CGS (centimeters, grams, seconds) units.

[1] presented more practical expressions for the determination of both permeability and skin factor:

$$\frac{k}{\mu_{eff}} = \left[70.6 (96681.605)^{(1-\alpha)(1-n)} \left(\frac{0.0002637 t_r}{n \phi c_t} \right)^\alpha \left(\frac{qB}{h} \right)^{n-\alpha(n-1)} \left(\frac{1}{(t^* \Delta P')_r} \right) \right]^{1-\alpha} \quad (14)$$

Where α is the slope of the pressure derivative curve and is defined by:

$$\alpha = \frac{1-n}{3-n} \quad (15)$$

$$s_{rNN} = \frac{1}{2} \left(\frac{(\Delta P)_{rNN}}{(t * \Delta P')_{rNN}} - \frac{1}{a} \right) \left(\frac{t_{rNN}}{G r_w^{3-n}} \right)^a \tag{16}$$

4. Well pressure behavior in non-Newtonian/Newtonian interface

In many activities of the oil industry, engineers have to deal with completion and stimulation treatment fluids such as polymer solutions and some heavy crude oils which obey a non-Newtonian power-law behavior. When it is required to conduct a treatment with a non-Newtonian fluid in an oil-bearing formation, this comes in contact with conventional oil which possesses a Newtonian nature. This implies the definition of two media with entirely different mobilities. If a pressure test is run in such a system, the interpretation of data from such a test through the use of conventional straight-line method may be erroneous and may not provide a way for verification of the results obtained. Then, [13] proposed a solution for the system sketched in Figure 3 which was solved numerically by [17].

[15] presented for the first time the pressure derivative behavior for the mentioned system, Figure 4. Notice in that plot that the pressure derivative shows an increasing slope as the flow behavior index decreases. Also, the derivative has no slope during infinite-acting Newtonian behavior, as expected.

During the non-Newtonian region, region 1 in Figure 3, Equations 13 to 15 work well. For the Newtonian region, region 2, the permeability and skin factor are estimated with the equations presented by Tiab (1993) as:

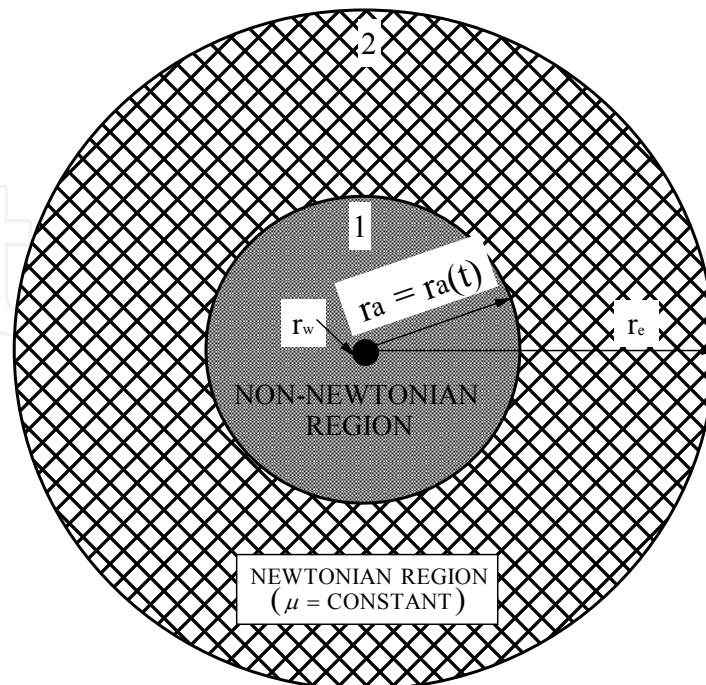


Figure 3. Composite non-Newtonian/Newtonian radial reservoir

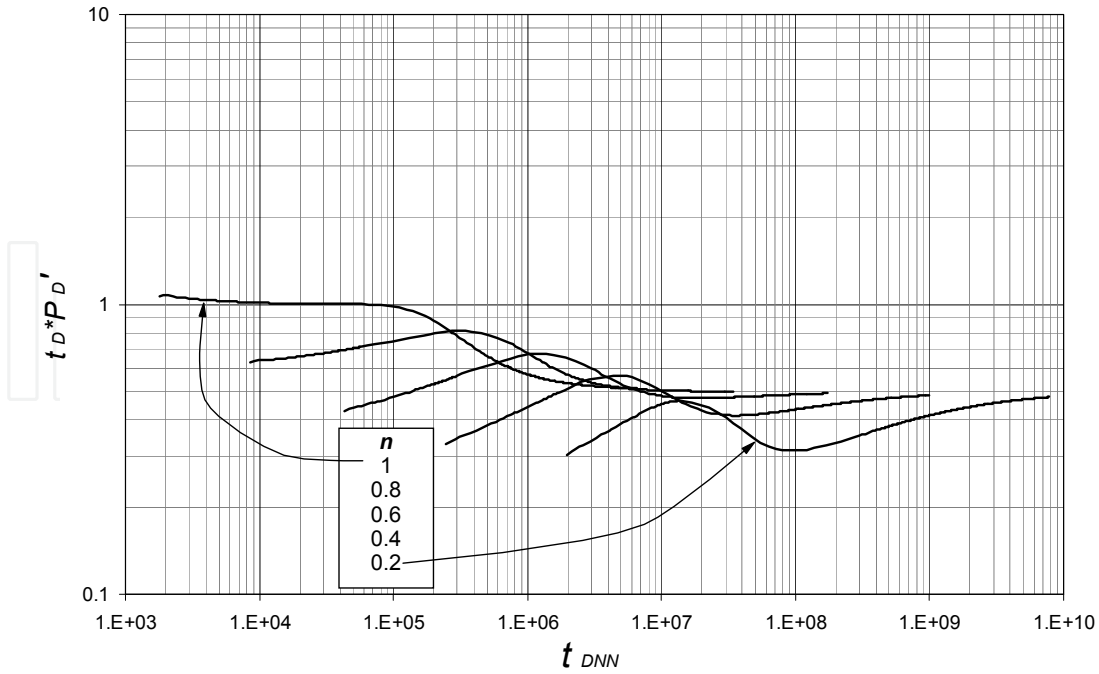


Figure 4. Dimensionless pressure derivative behavior for $r_a = 200$ ft. Case Non-Newtonian pseudoplastic

$$k_2 = \frac{70.6q\mu_N B}{h(t^* \Delta P')_r} \tag{17}$$

$$s_2 = \frac{1}{2} \left[\left(\frac{\Delta P}{t^* \Delta P'} \right)_{r_2} - \ln \left(\frac{k_2 t_{r_2}}{\phi \mu_N c_t r_w^2} \right) + 7.43 \right] \tag{18}$$

Suffix 2 denotes the non-Newtonian region.

[15] also found an expression to estimate the non-Newtonian permeability using the time of intersection of the non-Newtonian and Newtonian radial lines, t_{iN_NN} :

$$k = \left[\left\langle \left(\frac{H}{12} \right) \left(9 + \frac{3}{n} \right)^n \left(1.59344 \times 10^{-12} \phi \right)^{(1-n)/2} \left(96681.605 \frac{hr_w}{qB} \right)^{1-n} \right\rangle^{1-1/\alpha} \frac{\mu_N^{1/\alpha} \phi c_t r_w^2 n}{0.0002637 t_{iN_NN}} \right]^{1/2} \tag{19}$$

The radius of the injected non-Newtonian fluid bank is calculated using the following correlation (not valid for $n=1$), obtained from reading the time at which the pressure derivative has its maximum value:

$$r_a = \left[\frac{G \left(0.2258731n^3 - 0.2734284n^2 + 0.5064602n + 0.5178275 \right)^{1/\alpha}}{t_{MAX}} \right]^{1/(n-3)} \tag{20}$$

[13] found that the radius of the non-Newtonian fluid bank can be found using the radius investigation equation proposed by [10]:

$$r_a = \left[\Gamma \left(\frac{2}{3-n} \right) \right]^{1/(n-1)} \left[\frac{(3-n)^2 t}{G} \right]^{1/(3-n)} \tag{21}$$

where t is the end time of the straight line found on a non-Newtonian Cartesian graph of ΔP vs. $t^{1-n/3-n}$.

Later, [16] found that Equations 13, 14, 15 and 22 also worked for dilatant systems. This is the case when $2 < n < 1$. The pressure derivative behavior is given in Figure 5. Notice that for this case the slope decreases as the flow behavior index increases. For dilatant-Newtonian interface the position of the front obeys the following equation:

$$r_a = \left[\frac{G(0.46811e^{0.76241n})^{1/\alpha}}{t_{e_rNN}} \right]^{1/(n-3)} \tag{22}$$

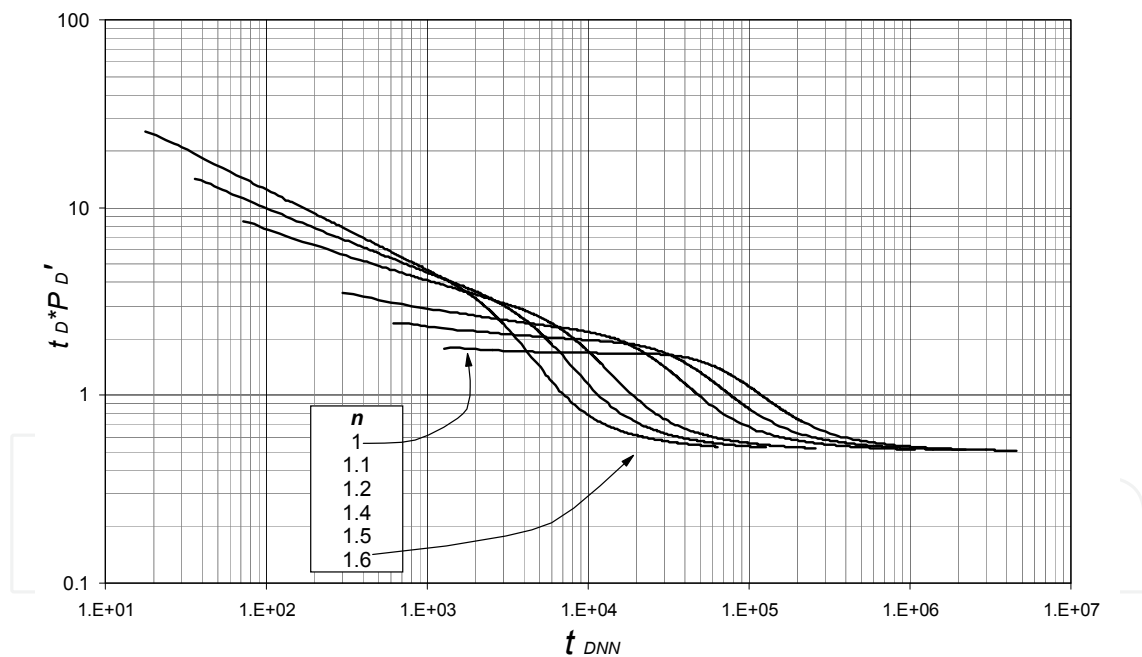


Figure 5. Dimensionless pressure derivative behavior for $r_a = 200$ ft. Case Non-Newtonian dilatant

Example 1. A constant-rate injection test for a well in a closed reservoir was generated by [13] with the data given below. It is required to estimate the permeability and the skin factor in each area and the radius of injected non-Newtonian fluid bank.

- | | | | |
|-----------------------------------|------------------|------------------------------|------------------|
| $P_R = 2500$ psi | $r_e = 2625$ ft | $r_w = 0.33$ ft | $h = 16.4$ ft |
| $\phi = 20$ % | $k = 100$ md | $q = 300$ BPD | $B = 1.0$ rb/STB |
| $c_t = 6.89 \times 10^{-6}$ 1/psi | $r_a = 131.2$ ft | $H = 20$ cp*s ⁿ⁻¹ | $\mu_N = 3$ cp |

$n = 0.6$

Solution. The log-log plot of pressure and pressure derivative against injection time is given in Figure 6. Suffix 1 and 2 indicate the non-Newtonian and Newtonian regions, respectively. From Figure 6 the following information was read:

$t_{r1} = 0.3$	$\Delta P_{r1} = 541.54$ psi	$(t^* \Delta P')_{r1} = 105.45$ psi
$t_{r2} = 120$	$\Delta P_{r2} = 991.5$ psi	$(t^* \Delta P')_{r2} = 39.02$ psi
$t_{MAX} = 1.3$	$t_{rN_NN} = 0.0008$ hr	

First, α is evaluated with Equation 15 to be 0.17 and a value of 100.4 md was found with Equation 14 for the non-Newtonian effective fluid permeability. Equation 4 is used to find an effective viscosity of 0.06465 cp(s/ft) ^{$n-1$} . Then, the skin factor in the non-Newtonian region is found with Equation 16 to be 179.7.

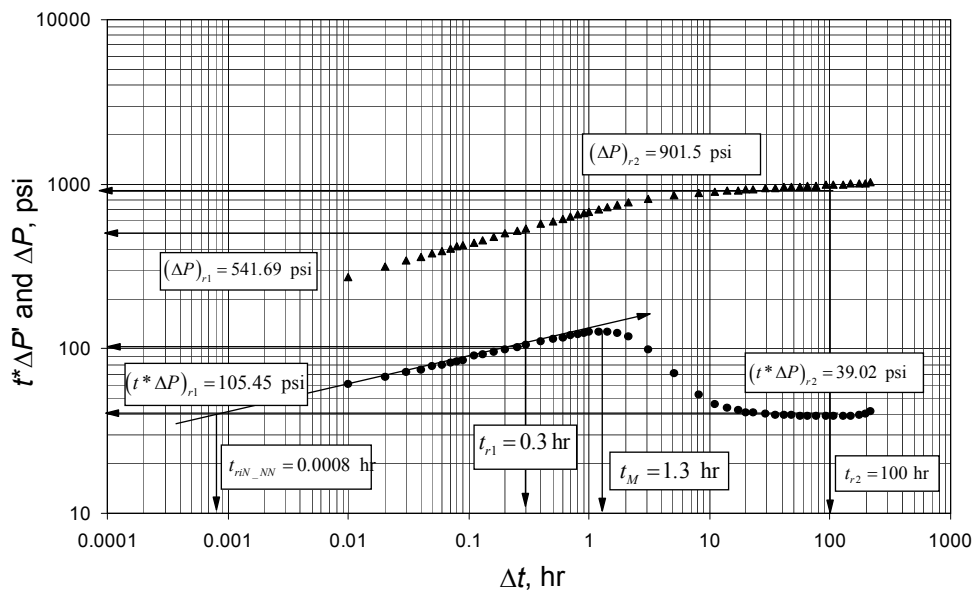


Figure 6. Pressure and pressure derivative for example 1

A value of 6.228×10^{-5} hr/(ft³⁻ⁿ) was found for parameter G using Equation 3. This value is used in Equation 24 to find the distance from the well to the non-Newtonian fluid bank. This resulted to be 120 ft.

Equations 17 and 18 were used to estimate permeability and skin factor of the Newtonian zone. They resulted to be 100 md and 4.5.

Using a time of 0.0008 hr which corresponds to the intersect point formed between the non-Newtonian and Newtonian radial flow regime lines in Equation 19, a non-Newtonian effective fluid permeability of 96 md is re-estimated. [13] obtained a permeability of the non-Newtonian zone of 101 md and $r_a = 116$ ft from conventional analysis.

5. Hydraulically fractured wells

[18] linearized the partial-differential equation for the problem of a well intercepted by a vertical fracture. Their dimensionless pressure solution is given below:

$$P_D(t_D) = \frac{(3-n)^{2\nu} t_D^\nu}{(1-n)\Gamma(1-\nu)} - \frac{1}{1-n} \quad (23)$$

Where $\nu = (1-n)/(3-n)$

[24] presented two interpretation methodologies: type-curve matching and conventional straight-line for characterization of fall-off tests in vertically hydraulic wells with a pseudoplastic fluid. They indicated that at early times, a well-defined straight line with slope equal to 0.5 on log-log coordinates will be evident, then,

$$P_D = \left(\frac{\pi}{2}\right)^{\frac{n-1}{2}} \sqrt{\pi^* t_{Dxf}} \quad (24)$$

$$t_{Dxf} = \frac{0.0002637kt}{\phi c_t \mu^* x_f^2} \quad (25)$$

Where the characteristic viscosity, μ^* , is given by:

$$\mu^* = \mu_{eff} \left(96681.605 \frac{h}{qB} \right)^{1-n} \quad (26)$$

And the derivative of Equation 24 is:

$$t_{Dxf} * P_D' = 0.5 \left(\frac{\pi}{2}\right)^{\frac{n-1}{2}} \sqrt{\pi t_{Dxf}} \quad (27)$$

And the dimensionless fractured conductivity is;

$$c_{fD} = \frac{k_f w_f}{k x_f} \quad (28)$$

[22] presented an expression which relate the half fracture length, x_f , formation permeability, k , fracture conductivity, $k_f w_f$, and post-frac skin factor, s :

$$k_f w_f = \frac{3.31739k}{\frac{e^s}{r_w} - \frac{1.92173}{x_f}} \quad (29)$$

However, there is no proof that Equation 28 works for Non-Newtonian systems. Using Equation 23, [3] presented pressure and pressure derivative curves for vertically infinite-conductivity fractured wells. See Figure 7. They extended the *TDS* methodology, [21], for the systems under consideration. By using the intersect point of the pressure derivatives during linear flow regime, Equation 26, with the radial flow regime governing equation, Equation 11, t_{RLi} , an expression to obtain the half-fracture length is presented:

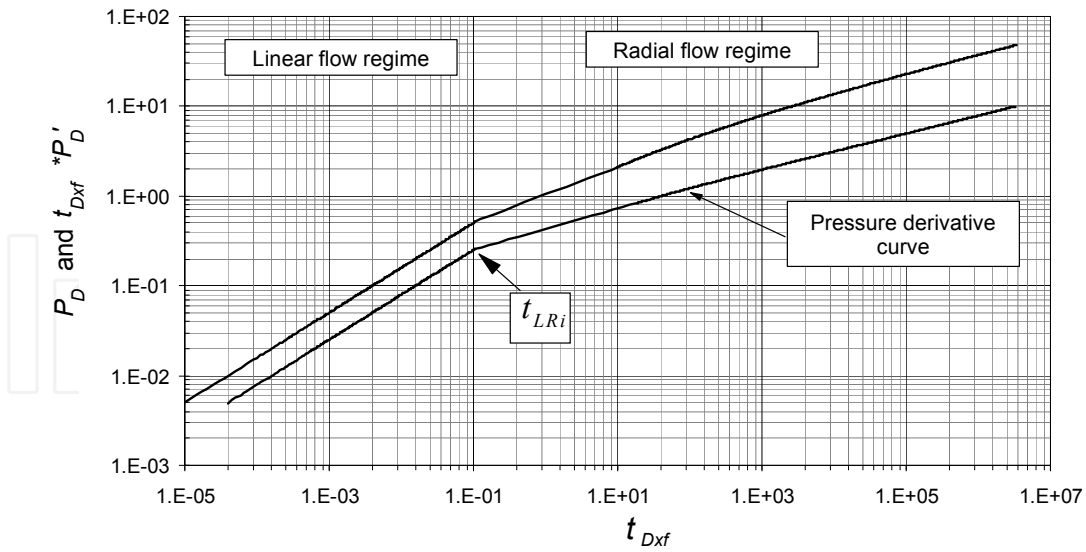


Figure 7. Dimensionless pressure and pressure derivative behavior for a vertical infinite-conductivity fractured well with a non-Newtonian pseudoplastic fluid with $n = 0.5$

$$x_f = \left[0.028783 \frac{(1.570796)^{\frac{n-1}{2}} \sqrt{t_{LRi} k}}{\left(\frac{0.0002637 k t_{LRi}}{\phi c_t \mu^*} \right)^\alpha \sqrt{\phi c_t \mu^*}} \right]^\alpha \quad (30)$$

Where $\nu = (1-n)/(3-n)$.

The expression governing the late-time pseudosteady-state flow regime is:

$$t_D^* P_D' = 2\pi t_{DA} \quad (31)$$

The point of intersection of the pressure derivatives during linear flow and pseudosteady-state (mathematical development is not shown here) allows to obtain the well drainage area by means of the following expression:

$$A = \pi \left[\frac{t_{iLPSS}}{0.0625 \left(\frac{\pi}{2} \right)^{n-1} G} \right]^{2/(3-n)} \quad (32)$$

Example 2. Fan (1998) presented a pressure test of a test conducted in a hydraulic fractured well with the information given below. Pressure and pressure derivative data for this test is reported in Figure 8.

$n = 0.4$	$h = 70 \text{ ft}$	$k = 0.65 \text{ md}$	$q = 507.5 \text{ BPD}$
$\phi = 10 \%$	$B = 1 \text{ rb/STB}$	$\mu^* = 0.00065 \text{ cp}$	$c_t = 0.00001 \text{ psi}^{-1}$

$r_w = 0.26 \text{ ft}$ $H = 20 \text{ cp}^* \text{s}^{n-1}$

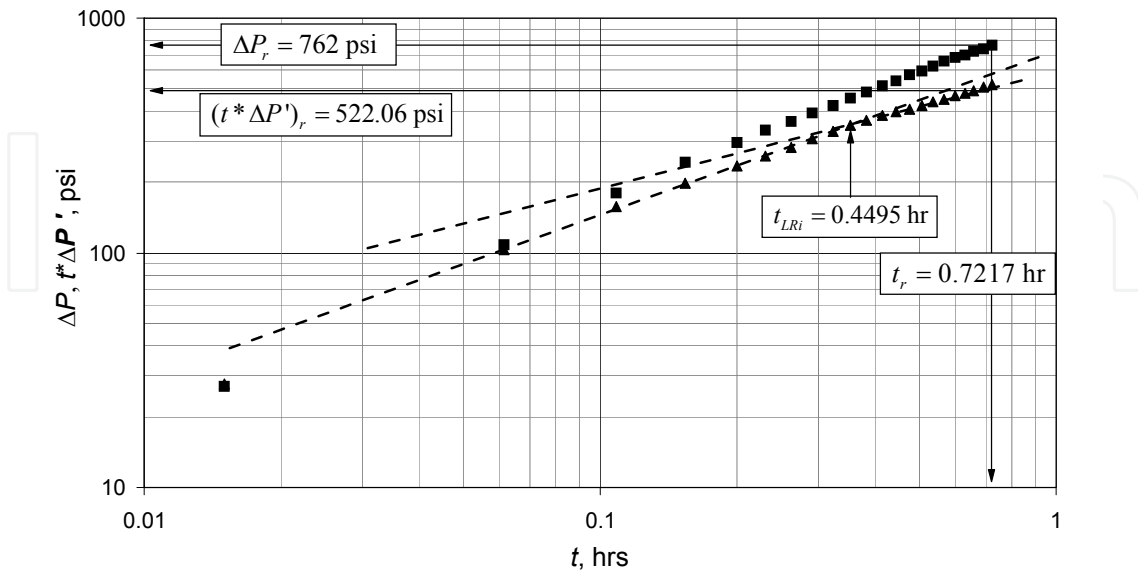


Figure 8. Pressure and pressure derivative for example 2

Solution. The following information was read from the pressure and pressure derivative plot, Figure 8,

$$t_{LRI} = 0.4495 \text{ hr} \qquad t_r = 0.7217 \text{ hr} \qquad \Delta P_r = 762 \text{ psi} \qquad (t^* \Delta P')_r = 522.06 \text{ psi}$$

Using Equation 15, a value of 0.23 is found for α . Reservoir permeability, skin factor, half-fracture length were estimated with Equations 14, 16 y 30. Their respective values are 0.65 md, -13.9 and 771 ft. Reservoir permeability and half-fracture length are re-estimate by simulating the test providing values of 0.65 md and 776 ft, respectively; therefore, the absolute errors for these calculations are less 0.06 % and 0.5 %. A G value of 0.001241 hr/(ft³⁻ⁿ) was found with Equation 3.

A fracture conductivity of 868.5 md-ft was calculated using Equation 29. It is important to clarify that this equation is valid for the Newtonian case. This value was used in Equation 28 to find a dimensionless fracture conductivity of 1.73.

6. Finite-homogeneous reservoirs

For the cases of bounded and constant-pressure reservoirs, [8] presented the solutions to Equation 1. The initial and boundary conditions for the first case are:

$$P_{DNN}(r_D, 0) = 0 \tag{33}$$

$$\left(\frac{\partial P_{DNN}}{\partial r_D} \right)_{r_D=1} = -1 \text{ for } t_{DNN} > 0 \tag{34}$$

$$\left(\frac{\partial P_{DNN}}{\partial r_D} \right)_{r_{eD}=1} = 0 \text{ for } t_{DNN} \tag{35}$$

The analytical solution in the Laplace space domain for the closed reservoirs under constant-rate case is given as:

$$\bar{P}(\bar{s}) = \frac{\left\{ K_{2/(3-n)} \left[\frac{2}{3-n} \sqrt{\bar{s}} r_{eD}^{(3-n)/2} \right] \bullet I_{1-n} \left[\frac{2}{3-n} \sqrt{\bar{s}} \right] + I_{2/(3-n)} \left[\frac{2}{3-n} \sqrt{\bar{s}} r_{eD}^{(3-n)/2} \right] \bullet K_{1-n} \left[\frac{2}{3-n} \sqrt{\bar{s}} \right] \right\}}{\left(\bar{s}^{3/2} \left\{ I_{2/(3-n)} \left[\frac{2}{3-n} \sqrt{\bar{s}} r_{eD}^{(3-n)/2} \right] \bullet K_{2/(3-n)} \left[\frac{2}{3-n} \sqrt{\bar{s}} \right] - K_{2/(3-n)} \left[\frac{2}{3-n} \sqrt{\bar{s}} r_{eD}^{(3-n)/2} \right] \bullet I_{2/(3-n)} \left[\frac{2}{3-n} \sqrt{\bar{s}} \right] \right\} \right)} \tag{36}$$

For the case of constant-pressure external boundary, the boundary condition given by Equation 35 is changed to:

$$P_{DNN}(r_{eD}, t_{DNN}) = 0 \tag{37}$$

And the analytical solution for such case is:

$$\bar{P}(\bar{s}) = \frac{\left\{ I_{1-n} \left[\frac{2}{3-n} \sqrt{\bar{s}} r_{eD}^{(3-n)/2} \right] \bullet K_{1-n} \left[\frac{2}{3-n} \sqrt{\bar{s}} \right] - K_{1-n} \left[\frac{2}{3-n} \sqrt{\bar{s}} r_{eD}^{(3-n)/2} \right] \bullet I_{1-n} \left[\frac{2}{3-n} \sqrt{\bar{s}} \right] \right\}}{\left(\bar{s}^{3/2} \left\{ I_{2/(3-n)} \left[\frac{2}{3-n} \sqrt{\bar{s}} \right] \bullet K_{1-n} \left[\frac{2}{3-n} \sqrt{\bar{s}} r_{eD}^{(3-n)/2} \right] + K_{2/(3-n)} \left[\frac{2}{3-n} \sqrt{\bar{s}} \right] \bullet I_{1-n} \left[\frac{2}{3-n} \sqrt{\bar{s}} r_{eD}^{(3-n)/2} \right] \right\} \right)} \tag{38}$$

Using the solution provided by [8], [4] presented pressure and pressure derivative plots for such behaviors as shown in Figs. 9 and 10. In these plots it is seen for closed systems in both pseudoplastic and dilatant cases, that the late-time pressure derivative behavior always displays a unit-slope line as for Newtonian fluids. As for Newtonian behavior, the late-time pressure derivative decreases in both dilatant or pseudoplastic cases.

[4] rewrote Equation 6 based on reservoir drainage area, so that:

$$t_{DA} = \frac{t}{G(\pi r_e^{3-n})} \tag{39}$$

[4] combined Equations 11, 31 and 39 to develop an analytical expression to find well drainage area,

$$A = \pi \left[\frac{t_{rpiNN}}{G} * \left(\frac{1}{4} \right)^{1/\alpha-1} \right]^{2/3-n} \tag{40}$$

Where t_{rpiNN} is the intersection point formed by the straight-lines of the radial and pseudosteady-state flow regimes. The above equation was multiplied by $(\pi^{(1/\alpha-1)})^{1/3-n}$ as a correction factor. This is valid for both dilatant and pseudoplastic non-Newtonian fluids.

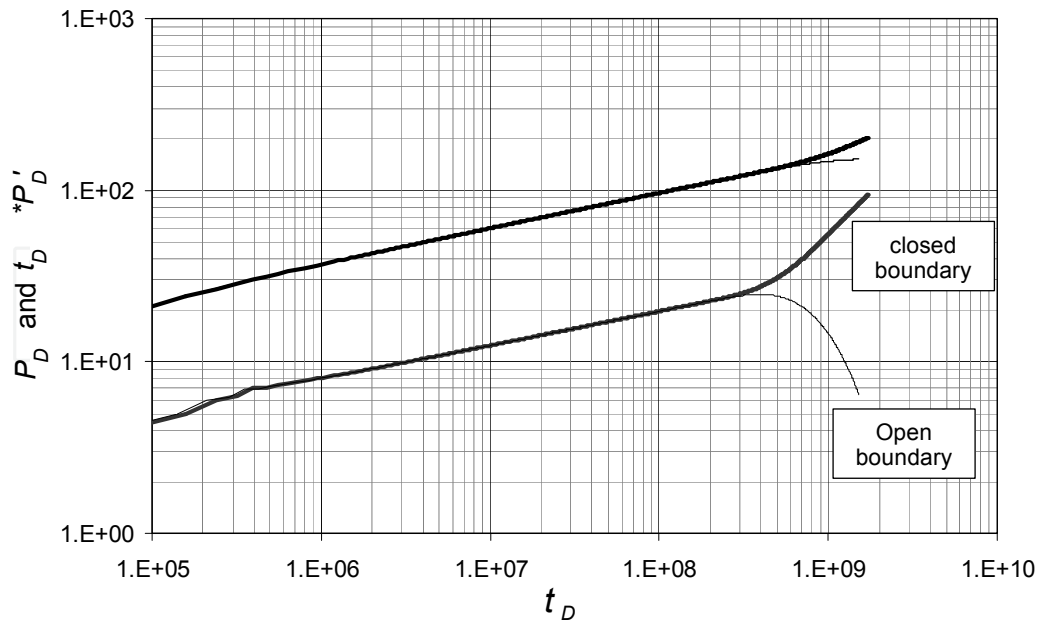


Figure 9. Dimensionless pressure and pressure derivative behavior in closed and open boundary systems for a non-Newtonian pseudoplastic fluid with $n = 0.5$, $r_e = 2000$ ft

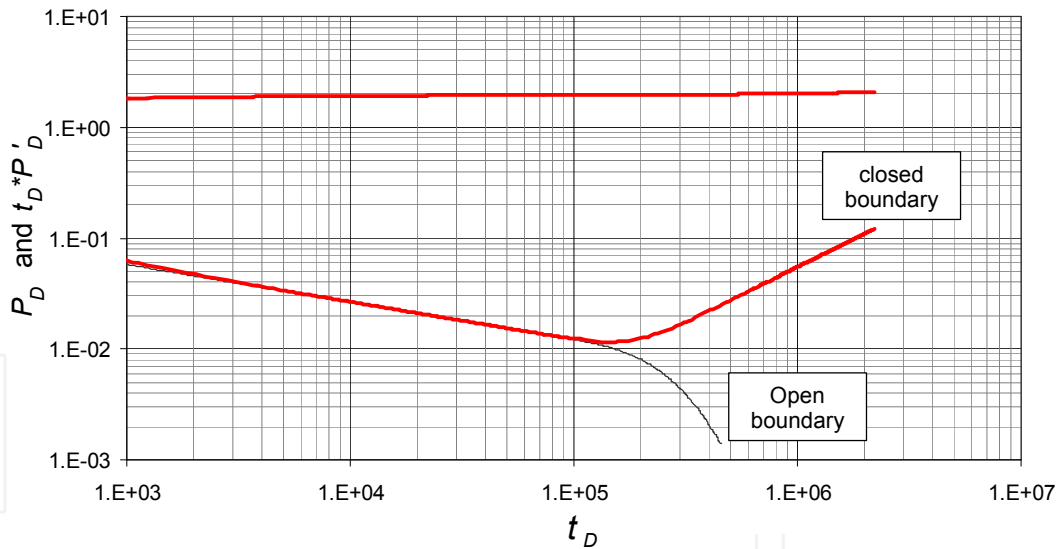


Figure 10. Dimensionless pressure and pressure derivative behavior in closed and open boundary systems for a non-Newtonian dilatant fluid with $n = 1.5$, $r_e = 2000$ ft

There is no pressure derivative expression for open boundary systems. Then, for pseudoplastic fluids the following correlation was also developed [4],

$$t_{DA_{NN}} = -0.003n^2 + 0.0337n + 0.052 \tag{41}$$

Equating Equation 41 to 39 and solving for reservoir drainage area, such as:

$$A = \pi \left[\frac{t_{rsiNN}}{G\pi(-0.003n^2 + 0.0337n + 0.052)} \right]^{\frac{2}{3-n}} \tag{42}$$

For dilatant fluids the correlation found is:

$$t_{DA_{NN}} = 0.9175n^3 - 3.7505n^2 + 5.1777n - 2.2913 \tag{43}$$

In a similar fashion as for the pseudoplastic case,

$$A = \pi \left[\frac{t_{rsiNN}}{G\pi(0.9175n^3 - 3.7505n^2 + 5.1777n - 2.2913)} \right]^{\frac{2}{3-n}} \tag{44}$$

t_{rsiNN} in Equations 42 and 44 corresponds is the intersection point formed by the straight-line of the radial and negative unit-slope line drawn tangentially to the steady-state flow regime.

Example 3. [4] presented a synthetic example to determine the well drainage area. Pressure and pressure derivative data are provided in Figure 11 and other relevant information is given below:

$n = 0.5$	$h = 16.4$ ft	$k = 350$ md	$q = 300$ BPD
$\phi = 5\%$	$B_o = 1$ rb/STB	$\mu_{eff} = 0.014833$ cp	$c_t = 0.0000689$ psi ⁻¹
$r_w = 0.33$ ft	$H = 20$ cp*s ⁿ⁻¹	$r_e = 2000$ ft	$P_i = 2500$ psi

Solution. From Figure 11, the intercept point, t_{rpiNN} , of the radial and pseudosteady-state straight lines is 60 hr which is used in Equation 40 to provide a well drainage area of 275 acres. Notice that this reservoir has an external radius of 2000 ft which represents an area of 288 acres. This allows obtaining an absolute error of 2.33 %.

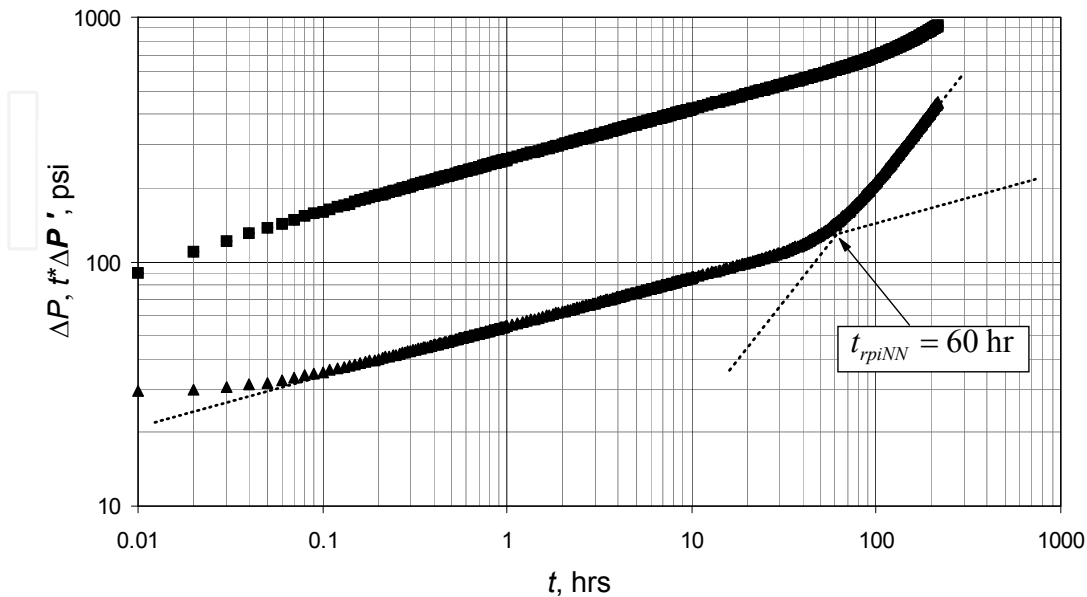


Figure 11. Pressure and pressure derivative for example 3

7. Heterogeneous reservoirs

In the well interpretation area of the Petroleum Engineering discipline a homogeneous reservoir is conceived to possess a single porous matrix while a heterogeneous reservoir has a porous matrix and either vugs or fractures. A common term used for heterogeneous systems is naturally-fractured reservoirs. However, this term is not recommended to be used since the fractures may result for either a mechanic process or a chemical process (matrix dissolution). Therefore, a more convenient term used in this book is double porosity systems in which the well is fed by the fractures and the fractures are fed by the matrix. By the same token, in a double-permeability system the well is fed by both fractures and matrix and the fractures are also fed by the matrix. This last one, however, has little application in the oil industry.

The governing well pressure solution in the Laplacian domain for a double-porosity system with a non-Newtonian fluid excluding wellbore storage and skin effects was provided by [19] as:

$$\tilde{P}_{DNN} = \frac{K_{1-n} \left(\frac{2}{3-n} \sqrt{\tilde{s}f(\tilde{s})} \right)}{\tilde{s} \left(\sqrt{\tilde{s}f(\tilde{s})} K_{\frac{2}{3-n}} \left(\frac{2}{3-n} \sqrt{\tilde{s}f(\tilde{s})} \right) \right)} \quad (45)$$

The Laplacian parameter, $f(\tilde{s})$ is a function of the model type and fracture system geometry and is given by:

$$f(s) = \frac{\omega(1-\omega)s + \lambda}{(1-\omega)s + \lambda} \quad (46)$$

[2] implemented the *TDS* methodology for characterization of double-porosity systems with pseudoplastic fluids. As for Newtonian case, the infinite-acting radial flow regime is represented by a horizontal straight line on the pressure derivative curve. The first segment corresponds to pressure depletion in the fracture network while the second portion is due to the pressure response of an equivalent homogeneous reservoir. On the other hand, the transition period which displays a trough on the pressure derivative curve during the transition period depends only on the dimensionless storage coefficient, ω . The Warren and Root parameters are defined in reference [26].

Figure 12 shows a log-log plot of the dimensionless pressure and pressure derivative for a double-porosity system with constant interporosity flow parameter, constant n value and variable dimensionless storage coefficient the higher ω the less pronounced the trough. As seen there, as the value of n decreases, the slope of the derivative during radial flow increases. In Figure 13 is shown the effect of variable of the interporosity flow parameter for constant values of dimensionless storage coefficient and flow behavior index. Notice in that

plot that as the value of λ decreases, the transition period shows up later. Finally, Figure 14 shows the effect of changing the value of the flow behavior index for constant values of λ and ω . The effect of the increasing the pressure derivative curve's slope is observed as the value of n decreases. Needless to say that neither wellbore storage nor skin effects are considered.

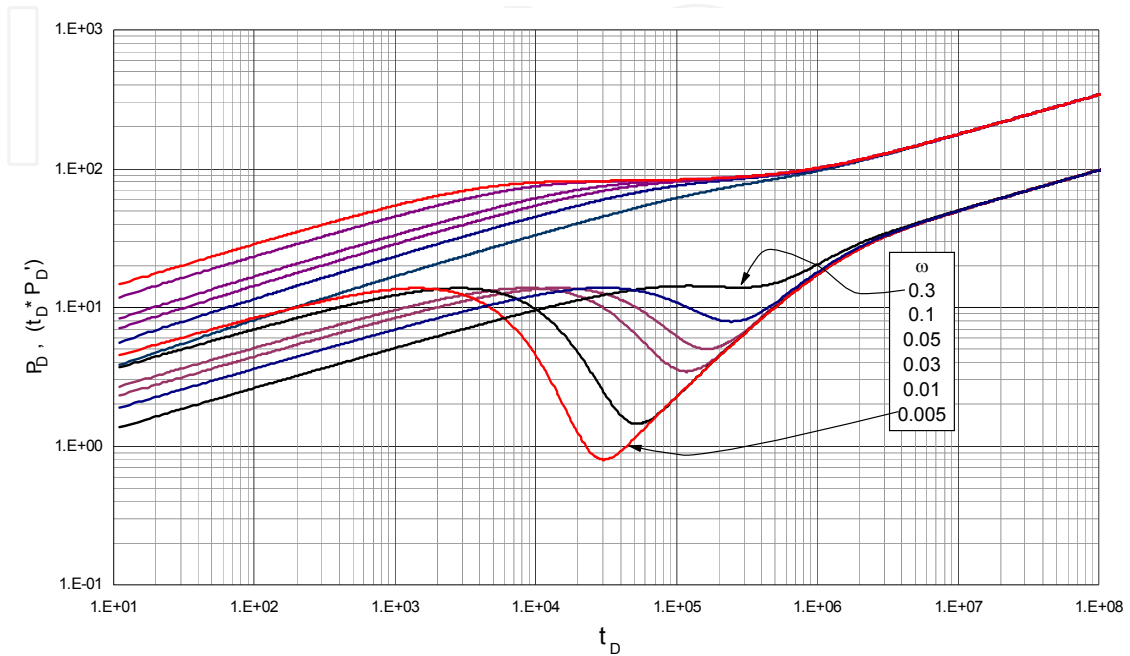


Figure 12. Dimensionless pressure and pressure derivative log-log plot for variable dimensionless storage coefficient, $\lambda=1 \times 10^{-6}$ and $n=0.2$ for a heterogeneous reservoir

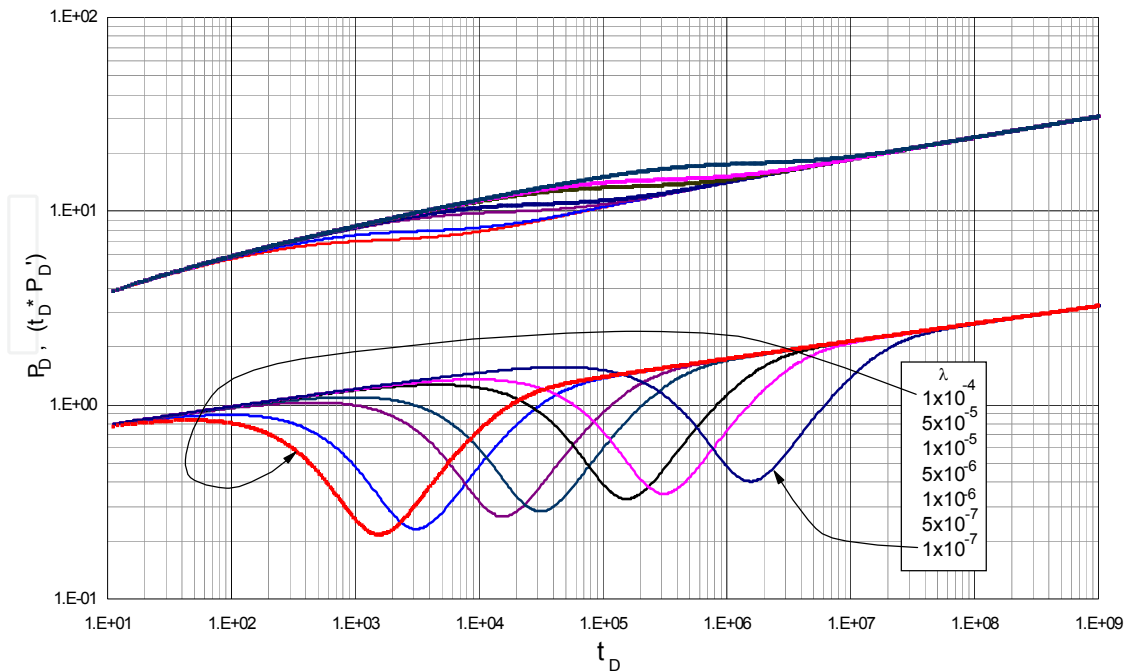


Figure 13. Dimensionless pressure and pressure derivative log-log plot for variable interporosity flow parameter, $\omega=0.05$ and $n=0.8$ for a heterogeneous reservoir

The infinite-acting radial flow regime is identified by a straight line which slope increase as the value of the flow behavior index decreases. See Figure 14. The first segment of such line corresponds to the fracture-network dominated period, and, the second one -once the transition effects are no longer present-, responds for a equivalent homogeneous reservoir. An expression for the slope is given [11] as:

$$m = \frac{n-1}{n-3} \tag{47}$$

Also, the slope of the pressure derivative during radial flow regime is related to the flow behavior index by:

$$n = -1.8783425 - 7.8618321m^3 + 0.19406557m^{0.5} + 2.8783425e^{-m} \tag{48}$$

As observed in Figure 12, as the dimensionless storage coefficient decreases the transition period is more pronounced no matter the value of the interporosity flow parameter. Therefore, a correlation for $0 \leq \omega \leq 1$ with an error lower than 3 % as a function of the minimum time value of the pressure derivative during the trough, the flow behavior index and the beginning of the second of the infinite-acting radial flow regime is developed in this study as:

$$\frac{1}{\omega} = \left| 3180.6369 + 551.0582 \left(\ln \frac{t_{\min}}{t_{b2}} \right)^2 - \frac{2053.5888}{x^{0.5}} + \frac{75.337547}{x} - \frac{1.4787073}{x^{1.5}} - \frac{910.05377}{n^{0.5}} + \frac{988.80592}{n} - \frac{459.61296}{n^{1.5}} + \frac{73.93695}{n^2} \right| \tag{49}$$

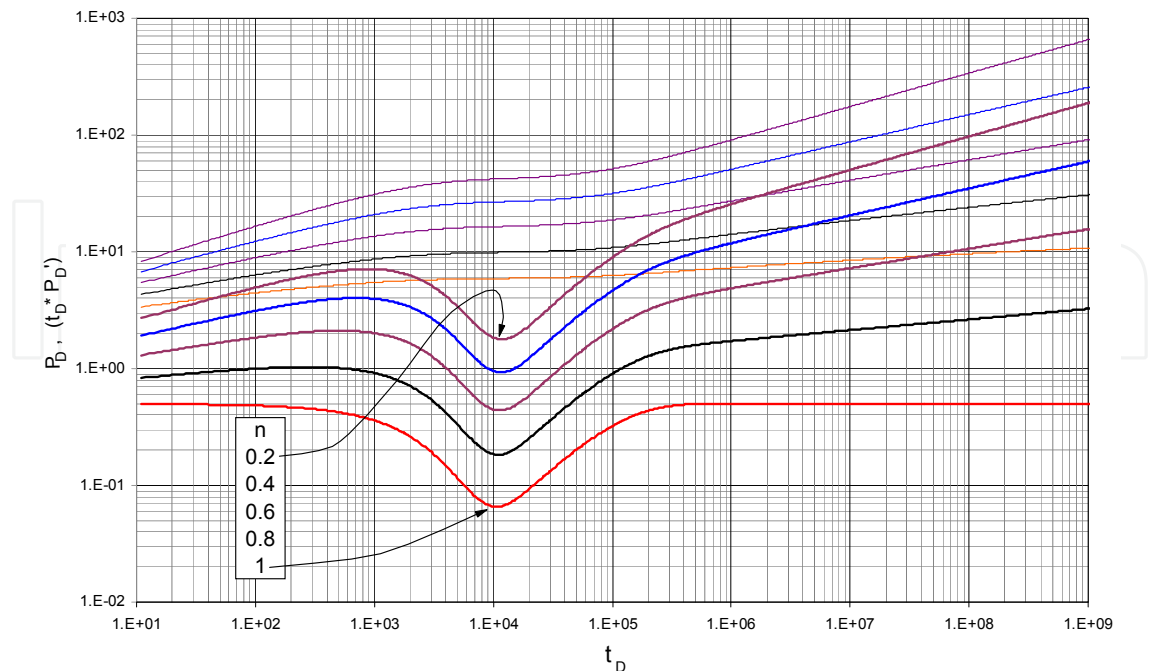


Figure 14. Dimensionless pressure and pressure derivative log-log plot for variable flow behavior index, $\omega=0.03$ and $\lambda=1 \times 10^{-5}$ for a heterogeneous reservoir

Another way to estimate ω uses a correlation which is a function of the intersection time between the unit-slope pseudosteady-state straight line developed during the transition period, the time of the trough. We also found that this correlation is also valid for $0 \leq \omega \leq 1$ with an error lower than 0.7 %.

$$\omega = 0.019884508 - \frac{1.153351}{y} + \frac{43.428536}{y^2} - \frac{555.85387}{y^3} + \frac{3232.6805}{y^4} - \frac{6716.9801}{y^5} - \frac{0.0093613189}{n} + \frac{0.0042870178}{n^2} + \frac{0.00027356586}{n^3} - \frac{0.0005221335}{n^4} + \frac{0.000072466135}{n^5} \quad (50)$$

A final correlation to estimate ω valid for $0 \leq \omega \leq 1$ with an error lower than 0.4 % is given as follows:

$$\omega = \frac{-0.098427346 + 0.00046337048y + 0.000025063353y^2 - 0.00000050316996y^3 + 0.0036057682n - 0.0073959605n^2}{1 - 0.36468068y - 0.064934748n - 0.047596083n^2} \quad (51)$$

The interporosity flow parameter also plays an important role in the characterization of double porosity systems. From Figure 13, it is observed that the smaller the value of λ the later the transition period to be shown up. A correlation for it was obtained using the time at the trough and the dimensionless storage coefficient, as presented by next expression:

$$\lambda = \frac{(6.9690127 \times 10^{-7} + 3.4893658 \times 10^{-8}n - 3.2315082 \times 10^{-8}n^2 - 5.9013807w + 21571690w^2 + 3.6102987 \times 10^{12}w^3)}{(1 + 0.0099353372n - 3740035.1w + 6.7143604 \times 10^{12}w^2)} \quad (52)$$

Equation 51 is valid for $1 \times 10^{-4} < \lambda < 9 \times 10^{-7}$ with an error lower than 4 %. A correlation involving the coordinates of the trough is given as:

$$\lambda = -0.00082917155 - 0.0014247498n - 0.00028717451z - 0.00077173053n^2 - 3.2538271 \times 10^{-5}z^2 - 0.0003203949nz - 0.0001423889n^3 - 1.212213 \times 10^{-6}z^3 - 1.7831692 \times 10^{-5}nz^2 - 8.6457217 \times 10^{-5}n^2z \quad (53)$$

Which is valid for $1 \times 10^{-4} < \lambda < 9 \times 10^{-7}$ with an error lower than 3.7 %. Another expression for λ within the same mentioned range involving the minimum time of the trough is given for an error lower than 1.3 %.

$$\ln \lambda = -2.1223034 - 0.09473309n + 0.077489686n^{0.5} \ln(n) - \frac{0.010651118}{n^{0.5}} - \frac{0.043958503}{w^{0.5}} + \frac{1.5653137 \times 10^{-5} \ln w}{w} + \frac{0.00024143014}{w} + \frac{8.7148736 \times 10^{-9}}{w^{1.5}} - \frac{4.0331364 \times 10^{-13}}{w^2} \quad (54)$$

Example 4. Figure 15 contains the pressure and pressure derivative log-log plot of a pressure test simulated by [2] with the information given below. It is requested to estimate from these data the dimensionless storage coefficient and the interporosity flow parameter.

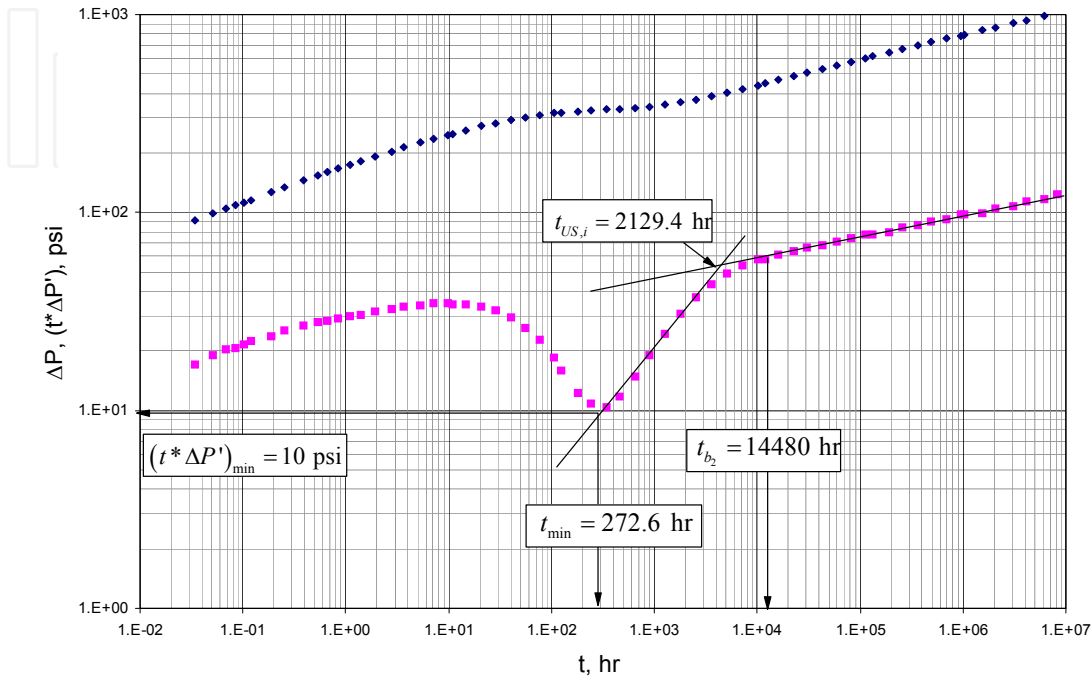


Figure 15. Pressure and pressure derivative for example 4

Solution. From Figure 15 the following characteristic points are read:

$$t_{min} = 272.6 \text{ hr} \quad t_{b2} = 14480 \text{ hr} \quad t_{US,i} = 2129.4 \text{ hr} \quad (t^* \Delta P')_{min} = 10 \text{ psi}$$

Using Equations 5 and 6, the above data are transformed into dimensionless quantities as follows:

$$t_{Dmin} = 32000 \quad t_{Db2} = 17000000 \quad t_{DUS,i} = 250000 \quad (t^* P_{D'})_{min} = 0.31$$

During the infinite-acting radial flow regime the following points were arbitrarily read:

$$(t)_{r1} = 35724.9 \text{ hr} \quad (t^* \Delta P')_{r1} = 67.292 \text{ psi} \quad (t)_{r2} = 56169.5 \text{ hr} \quad (t^* \Delta P')_{r2} = 61.2283 \text{ psi}$$

With these points a slope is estimated to be $m = 0.108$. Equation 47 allows obtaining a flow behavior index of 0.76. The Warren and Root's naturally fractured reservoir parameters are estimated as follows:

Equation	ω	Equation	λ
49	0.052	52	5.01E-06
50	0.05	53	5.043E-06
51	0.05	54	3.66E-06

Table 1. Summary of results for example 4

As a final remark, I would like to comment that some crude oils or other type of fluids used in the oil industry may display a non-Newtonian Bingham-type behavior. It is common to deal with Non Newtonian fluids during fracturing and drilling operations and oil recovery processes, as well. When a reservoir contains a non-Newtonian fluid, such as those injected during EOR with polymers flooding or the production of heavy-oil, the interpretation of a pressure test for these systems cannot be conducted using the conventional models for Newtonian fluid flow since it will lead to erroneous results due to a completely different behavior.

The problem considered now, presented in reference [27], involves the production of a Bingham fluid from a fully penetrating vertical well in a horizontal reservoir of constant thickness; the formation is saturated only with the Bingham fluid. The basic assumptions are: (a) Isothermal, isotropic and homogeneous formation, (b) Single-phase horizontal flow without gravity effects, (c) Darcy's law applies, and (d) Constant fluid properties and formation permeability.

The governing flow equation can be derived by combining the modified Darcy's law with the continuity equation and is expressed in a radial coordinate system as:

$$\frac{k}{r} \frac{\partial}{\partial r} \left[\frac{\rho(P)}{\mu_B} r \left(\frac{\partial P}{\partial r} - G \right) \right] = \frac{\partial}{\partial t} [\rho(P)\phi(P)] \quad (55)$$

The density of the Bingham fluid, $\rho(P)$, and the porosity of the formation, $\phi = \phi(P)$, are functions of pressure only, so Equation 54 may be rewritten as:

$$\frac{1}{r} \frac{\partial}{\partial r} \left[r \left(\frac{\partial P}{\partial r} - G \right) \right] = \frac{\phi \mu_B c_t}{k} \frac{\partial P}{\partial t} \quad (56)$$

The initial condition is:

$$P(r, t = 0) = P_i, \quad r \geq r_w \quad (57)$$

At the wellbore inner boundary, $r = r_w$, the fluid is produced at a given production rate, q ; then, the inner boundary condition is:

$$q = 2\pi r h \frac{k}{\mu_B} \left(\frac{\partial P}{\partial r} - G \right)_{r=r_w} \quad (58)$$

Parameter G is the minimum pressure gradient which expressed in dimensionless form yields:

$$G_D = \frac{G r_w k h}{141.2 q \mu_B B} \quad (59)$$

[15] solved numerically Equation 55 and provided an interpretation technique for this type of fluids using the pressure and pressure derivative log-log plot. For a Bingham-type non-Newtonian fluid, this behavior changes by observing that there is a point where the dimensionless pressure derivative is high and this increases with an increase of G_D and the reservoir radius, Figure 16.

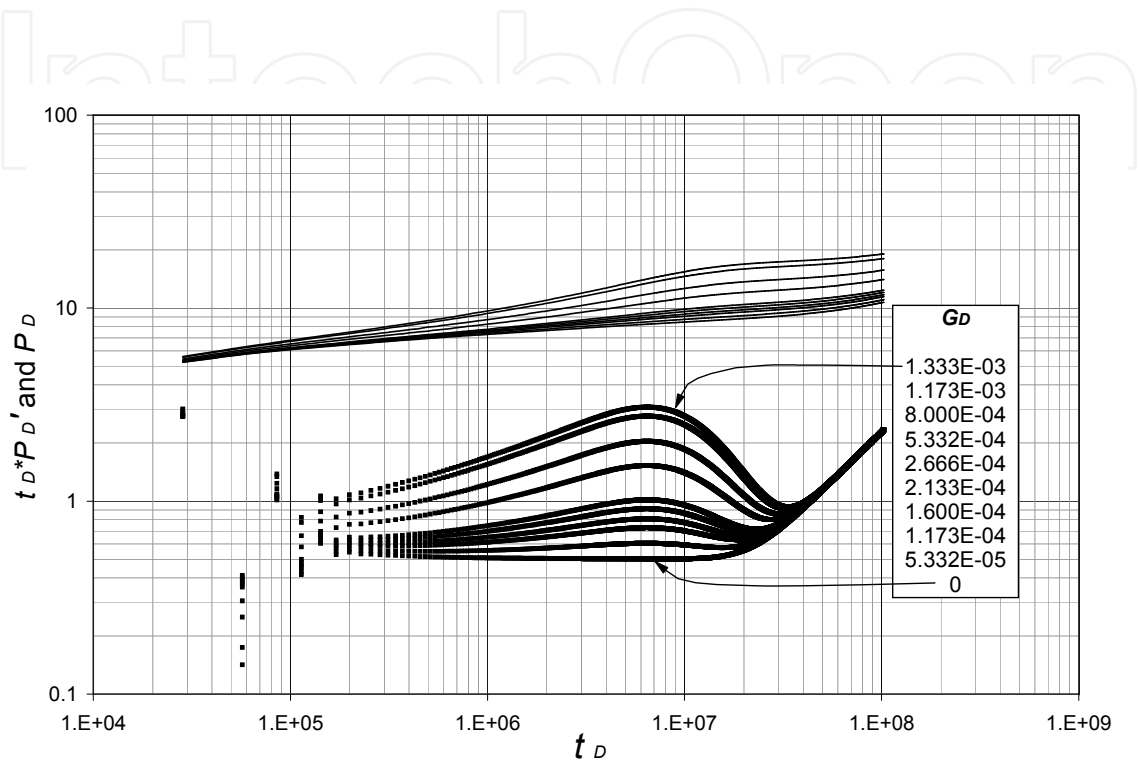


Figure 16. Dimensionless pressure and derivative pressure for $r_{eD} = 9375$

8. Conclusion

This chapter comprises the most updated state-of-the-art for well test interpretation in reservoirs having a non-Newtonian fluid. Extension of the *TDS* technique along with practical examples is given for demonstration purposes. This should be of extreme importance since most heavy oil fluids behave non-Newtonianly, then, its characterization using conventional analysis is inappropriate and the methodology presented here are strongly recommended.

Nomenclature

B	Volumetric factor, RB/STB
c_t	System total compressibility, 1/psi
C	Wellbore storage, bbl/psi
C_{fD}	Dimensionless fracture conductivity

h	Formation thickness, ft
H	Consistency (Power-law parameter), $\text{cp}^*\text{s}^{n-1}$
G	Group defined by Equation 3
G	Minimum pressure gradient, Psi/ft
G_D	Dimensionless pressure gradient
k	Permeability, md
k	Flow consistency parameter
k_{fwf}	Fracture conductivity, md-ft
m	Slope
n	Flow behavior index (power-law parameter)
P	Pressure, psi
q	Flow/injection rate, STB/D
t	Time, hr
r	Radius, ft
$t^*\Delta P'$	Pressure derivative, psi
$t_D^*P_D'$	Dimensionless pressure derivative
r_a	Distance from well to non-Newtonian/Newtonian front/interface
w	ω/t_{Dmin}
\tilde{S}	Laplace parameter
x	t_{min}/t_{b2}
x_f	Half-fracture length, ft
y	t_{USi}/t_{min}
z	$\ln [(t_D^*P_D')_{min}/t_{Dmin}]$

Table 2. Nomenclature of main variables

Δ	Change, drop
ϕ	Porosity, Fraction
γ	Shear rate, s^{-1}
σ	Shear stress, N/m
λ	Dimensionless interporosity parameter
μ	Viscosity, cp
μ_{eff}	Effective viscosity for power-law fluids, $\text{cp}^*(\text{s}/\text{ft})^{n-1}$
μ_B	Bingham plastic coefficient, cp
μ^*	Characteristic viscosity, $\text{cp}/\text{ft}^{1-n}$
τ	Shear stress, N/m
ω	Dimensionless storativity coefficient

Table 3. Greeks

1	Non-Newtonian region
2	Newtonian region
<i>app</i>	Apparent
<i>D</i>	Dimensionless
<i>DA</i>	Dimensionless based on area Based on area
<i>Dxf</i>	Dimensionless based on half-fracture length Based on area
<i>e</i>	External
<i>eff</i>	Effective
<i>i</i>	Initial
<i>LPi</i>	Intersect of linear and pseudosteady-state lines
<i>M</i>	Maximum
<i>N</i>	Newtonian
<i>NN</i>	Non-Newtonian
<i>r</i>	Radial (any point on radial flow)
<i>RLi</i>	Intersect of radial and linear lines
<i>rpiNN</i>	Intersect of radial and pseudosteady-state lines
<i>rsiNN</i>	Intersect of radial and steady-state lines
<i>w</i>	Wellbore

Table 4. Suffices

Author details

Freddy Humberto Escobar

Universidad Surcolombiana, Neiva (Huila), Colombia, South America

9. References

- [1] Escobar, F.H., Martinez, J.A., and Montealegre-M., Matilde, 2010. Pressure and Pressure Derivative Analysis for a Well in a Radial Composite Reservoir with a Non-Newtonian/Newtonian Interface. CT&F. Vol. 4, No. 1. p. 33-42. Dec. 2010.

- [2] Escobar, F.H., Zambrano, A.P, Giraldo, D.V. and Cantillo, J.H., 2011. Pressure and Pressure Derivative Analysis for Non-Newtonian Pseudoplastic Fluids in Double-Porosity Formations. CT&F, Vol. 5, No. 3. p. 47-59. June.
- [3] Escobar, F.H., Bonilla, D.F. and Ciceri, Y,Y. 2012. Pressure and Pressure Derivative Analysis for Pseudoplastic Fluids in Vertical Fractured wells. Paper sent to CT&F to request publication.
- [4] Escobar, F.H., Vega, L.J. and Bonilla, L.F., 2012b. Determination of Well Drainage Area for Power-Law Fluids by Transient Pressure Analysis". Paper sent to CT&F to request publication.
- [5] Fan, Y. 1998. A New Interpretation Model for Fracture-Calibration Treatments. SPE Journal. P. 108-114. June.
- [6] Hirasaki, G.J. and Pope, G.A., 1974. Analysis of Factors Influencing Mobility and Adsorption in the Flow of Polymer Solutions through Porous Media. Soc. Pet. Eng. J. Aug. 1974. p. 337-346.
- [7] Igbokoyi, A. and Tiab, D., 2007. New type curves for the analysis of pressure transient data dominated by skin and wellbore storage: Non-Newtonian fluid. Paper SPE 106997 presented at the SPE Production and Operations Symposium, 31 March – 3 April, 2007, Oklahoma City, Oklahoma.
- [8] Ikoku, C.U. 1978. Transient Flow of Non-Newtonian Power-Law Fluids in Porous Media. Ph.D. dissertation. Stanford U., Stanford, CA.
- [9] Ikoku, C.U., 1979. Practical Application of Non-Newtonian Transient Flow Analysis. Paper SPE 8351 presented at the SPE 64th Annual Technical Conference and Exhibition, Las Vegas, NV, Sept. 23-26.
- [10] Ikoku, C.U. and Ramey, H.J. Jr., 1979. Transient Flow of Non-Newtonian Power-law fluids Through in Porous Media. Soc. Pet. Eng. Journal. p. 164-174. June.
- [11] Ikoku, C.U. and Ramey, H.J. Jr., 1979. Wellbore Storage and Skin Effects During the Transient Flow of Non-Newtonian Power-law fluids Through in Porous Media. Soc. Pet. Eng. Journal. p. 164-174. June.
- [12] Katime-Meindl, I. and Tiab, D., 2001. Analysis of Pressure Transient Test of Non-Newtonian Fluids in Infinite Reservoir and in the Presence of a Single Linear Boundary by the Direct Synthesis Technique. Paper SPE 71587 prepared for presentation at the 2001 SPE Annual Technical Conference and Exhibition held in New Orleans, Louisiana, 30 Sept.–3 Oct.
- [13] Lund, O. and Ikoku, C.U., 1981. Pressure Transient Behavior of Non-Newtonian/Newtonian Fluid Composite Reservoirs. Society of Petroleum Engineers of AIME. p. 271-280. April.
- [14] Mahani, H., Sorop, T.G., van den Hoek, P.J., Brooks, A.D., and Zwaan, M. 2011. Injection Fall-Off Analysis of Polymer Flooding EOR. Paper SPE 145125 presented at the

- SPE Reservoir Characterization and Simulation Conference and Exhibition held in Abu Dhabi, UEA, October 9-11.
- [15] Martinez, J.A., Escobar, F.H., and Montealegre-M, M. 2011. Vertical Well Pressure and Pressure Derivative Analysis for Bingham Fluids in a Homogeneous Reservoirs. *Dyna*, Year 78, Nro. 166, p.21-28. *Dyna*. 2011.
- [16] Martinez, J.A., Escobar, F.H. and Cantillo, J.H., 2011b. Application of the TDS Technique to Dilatant Non-Newtonian/Newtonian Fluid Composite Reservoirs. Article sent to *Ingeniería e Investigación* to request publication. *Ingeniería e Investigación*. Vol. 31. No. 3. P. 130-134. Aug.
- [17] Martinez, J.A., Escobar, F.H. and Bonilla, L.F. 2012. "Numerical Solution for a Radial Composite Reservoir Model with a Non-Newtonian/Newtonian Interface. Paper sent to CT&f to request publication.
- [18] Odeh, A.S. and Yang, H.T., 1979. Flow of non-Newtonian Power-Law Fluids Through in Porous Media. *Soc. Pet. Eng. Journal*. p. 155-163. June.
- [19] Olarewaju, J.S., 1992. A Reservoir Model of Non-Newtonian Fluid Flow. SPE paper 25301.
- [20] Savins, J.G., 1969. Non-Newtonian flow Through in Porous Media. *Ind. Eng. Chem.* 61, No 10, Oct. 1969. p. 18-47.
- [21] Tiab, D., 1993. Analysis of Pressure and Pressure Derivative without Type-Curve Matching: 1- Skin and Wellbore Storage. *Journal of Petroleum Science and Engineering*, Vol 12, pp. 171-181. Also Paper SPE 25423, Production Operations Symposium held in Oklahoma City, OK. pp 203-216.
- [22] Tiab, D., Azzougen, A., Escobar, F. H., and Berumen, S. 1999. "Analysis of Pressure Derivative Data of a Finite-Conductivity Fractures by the 'Direct Synthesis Technique'." Paper SPE 52201 presented at the 1999 SPE Mid-Continent Operations Symposium held in Oklahoma City, OK, March 28-31, 1999 and presented at the 1999 SPE Latin American and Caribbean Petroleum Engineering Conference held in Caracas, Venezuela, 21-23 April.
- [23] van Poollen, H.K., and Jargon, J.R. 1969. Steady-State and Unsteady-State Flow of Non-Newtonian Fluids Through Porous Media. *Soc. Pet. Eng. J.* March 1969. p. 80-88; *Trans. AIME*, 246.
- [24] Vongvuthipornchai, S. and Raghavan, R. 1987. Pressure Falloff Behavior in Vertically Fractured Wells: Non-Newtonian Power-Law Fluids. *SPE Formation Evaluation*, December, p. 573-589.
- [25] Vongvuthipornchai, S. and Raghavan, R. 1987b. Well Test Analysis of Data Dominated by Storage and Skin: Non-Newtonian Power-Law Fluids. *SPE Formation Evaluation*, December, p. 618-628.
- [26] Warren, J.E. and Root, P.J. 1963. The Behavior of Naturally Fractured Reservoirs. *Soc. Pet. Eng. J.* (Sept. 1963): 245-255.

- [27] WU, Y.S., 1990. Theoretical Studies of Non-Newtonian and Newtonian Fluid Flow Through Porous Media. Ph.D. dissertation, U. of California, Berkeley.

IntechOpen

IntechOpen